Dynamic Imaging of Carbon Nanotube - Liquid Crystal Suspensions

Raymond Bjorkman

Senior Thesis, Mechanical Engineering

Tufts University
School of Engineering
Medford, Massachusetts
May 16, 2015

Research Advisor:_____
Assistant Professor Jeffrey S. Guasto
Tufts University

Committee:_____
Assistant Professor Timothy J. Atherton
Tufts University

Abstract

Liquid crystals (LCs) are materials that exhibit fluid-like properties, while maintaining a degree of long-range crystalline order. They exhibit a variety of useful electro-optical properties and have found wide use in liquid crystal displays, optical telecommunications, and soft actuators. The speed at which the material responds to an applied electric field (switching speed) is a critical determinant of device performance. To study the spatiotemporal dynamics of LC materials, a novel method combining high-speed imaging with polarized light microscopy was developed, which provides micron spatial resolution and millisecond temporal resolution. This method was validated by quantifying the switching dynamics of a well-characterized liquid crystal (5CB) in a canonical Fréedericksz cell geometry. High-speed polarization microscopy was then applied to measure the effect of carbon nanotube (CNT) dopants on LC switching dynamics. CNTs are found to reduce the switching speed by about 10% compared to pure 5CB liquid crystal over voltages ranging from 2.5 – 3.5V.

Table of Contents

1. Introduction

Liquid crystals (LCs) are materials often comprised of elongated molecules, which can exist as solids, liquids, or an intermediate LC phase (Figure 1). In this phase, LC molecules are loosely organized and can flow under applied stress as a fluid. The LC molecules simultaneously show a degree of long-range orientational order. The ordering and anisotropy of LCs confers interesting and useful optical properties that can be controlled by manipulating their microstructure through applied electric fields. Such electro-optical properties make LCs incredibly useful to a range of optical technologies including the multi-billion-dollar liquid crystal display (LCD) industry.[1] Liquid crystals are also prominently used in the telecommunications industry as optical switches,[2] and show promise as mechanical actuators in the budding field of soft robotics.[3]

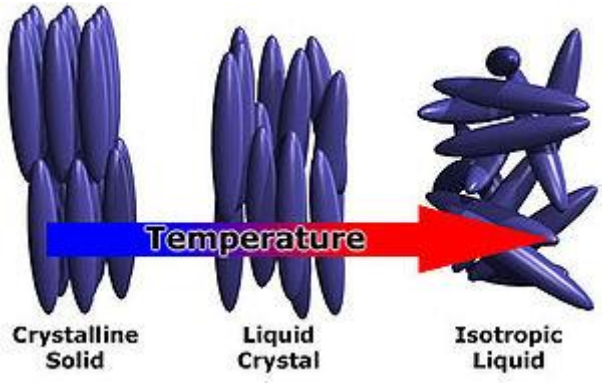

Figure 1 – Visualization of the Liquid Crystal Phase: The LC phase exists between the solid and liquid phases. This phase shows a degree of orientational order like a solid, but exhibits the ability to flow like a liquid. Image source: http://photonicswiki.org/index.php?title=Liquid_Crystals

LCDs are used in favor of other display technologies such as Cathode Ray Tubes (CRTs) and Plasma displays for their low cost, power consumption, and form factor while retaining high image quality. Compared to CRTs, however, LCDs are lagging behind in video refresh rate.[4] In every application of LCs, system performance depends on the speed at which the LC material can respond to applied electrical signals. In the display industry, a faster switching LC device

translates to faster frame rates. Additionally, high quality LC devices require spatial uniformity in the LC response.

One of the primary engineering challenges for designing faster LC devices is the need for a diagnostic method to characterize both spatial and temporal switching dynamics simultaneously. Analytical models and numerical simulations can yield predictions regarding LC behavior, but they must be grounded in empirical data. Therefore, this type of dynamic analysis has historically been done through capacitive sensing which has high temporal, but no spatial resolution. Conversely, confocal microscopy has been used to achieve very accurate spatial measurements at the expense of temporal resolution. The high-speed polarized light microscopy method presented here, provides a simple and elegant method by which complex spatial and temporal dynamics can be measured.

The efficacy of this method was demonstrated by quantifying the dynamics of pure LCs subject to a variety of different electrical stimuli in a Fréedericksz cell, to establish a performance baseline. Subsequently, this method was applied to characterize the dynamics of carbon nanotube (CNT) doped LC and compared to pure LC to determine the net effect of CNTs on the LC switching speed. The performance effects of doping LCs with CNT particles have not been fully studied yet, but some research has suggested that the study of doping LCs with CNTs could improve LCD technology.[5] This paper will investigate these claims using this newly developed experimental method.

2. Background

2.1 Properties of Liquid Crystal

Liquid crystals represent a phase of material having properties between solid and liquid phases. While LCs can further be subdivided into more specific phases, this research will focus on the properties of 4-Cyano-4'-pentylbiphenyl (5CB), which exhibits the nematic liquid crystalline phase. The nematic phase is fluid-like having properties such as viscosity, but also solid-like due to the long range orientational order exhibited by the molecules. That is, LCs retain a semi-ordered bulk material structure, like the crystal lattice structure of solids.[6]

These interesting properties can be explained because molecules comprising a LC are often anisotropic and have directionality in their shape and dielectric constant. LC molecules are non-spherical and are often considered "rod-like" or ellipsoidal in geometry, having a long axis and a short axis. Individual 5CB molecules have a length scale on the order of nanometers. When these molecules form the nematic LC phase, this anisotropy is carried over and the bulk material exhibits long-range orientational order.[2] The vector $\hat{n}$ defines the average orientation of the bulk LC and is called the director. The degree to which the molecules point in the same direction is called the order parameter, S. The order parameter is expressed by the following equation, where θ is the angle between $\hat{n}$ and the long axis of a molecule, and angled brackets denote an average over many molecules:

$$S = \frac{1}{2}\langle 3\,cos^2\,\theta - 1\rangle$$

Additionally, these molecules are polarized and have unbalanced charge along its long axis. The dielectric constants can be broken up into two parts, parallel $\varepsilon_{\parallel}$ and perpendicular $\varepsilon_{\perp}$ to the long axis of the molecule.[6] Dielectric anisotropy $\Delta\varepsilon$ is achieved when the parallel dielectric constant is larger than the perpendicular direction, such that $\varepsilon_{\parallel} > \varepsilon_{\perp}$. 5CB has a comparatively

large anisotropy, with $\varepsilon_{\parallel} = 18.5$ and $\varepsilon_{\perp} = 7$.[7] Dielectric anisotropy in LC molecules implies that when an electric field is applied, the molecules will feel a torque such that they rotate until the director aligns with the field, in a process referred to as "switching" (or switch-on). When the applied electric field is removed, the LC will revert to its original state in a second process called relaxation (or switch-off). The switching of LCs from one state to another due to the presence of an external electric field is the basis for LC dynamics.

While the ability of this class of material to shift in response to an external field is interesting in itself, it becomes incredibly useful when considered in conjunction with birefringence. Birefringence is an optical material property in which incident light is subject to different refractive indices when passing through a substrate. The bulk anisotropy of LCs is responsible for birefringent effects and causes two refractive indices called the ordinary and extraordinary indices and is denoted as n_o and n_e respectively. The extraordinary axis lies along the long axis, with the ordinary axis perpendicular to that. Light passing through a LC medium can be separated into components along the ordinary and extraordinary axes, with the respective indices acting on each component. Thus, light entering the medium with one polarization state will have its polarization state altered as its components are changed when passing through the LC. The birefringence of a material is commonly described by the difference between the extraordinary and ordinary indices of refraction:[6]

$$\Delta n = n_e - n_o$$

Additionally, the rate of phase change of the light during this transition can be expressed with respect to the distance the light has traveled through a LC medium, x, by the equation:

$$\frac{d\phi}{dx} = -\frac{2\pi}{\lambda}\Delta n$$

Because LCs are able to alter the polarization state of light depending on their orientation, they function as variable phase retarders. Conversely, the orientation of the LCs can be probed by interrogating the change in polarization state of light with a known incident polarization, for example with a crossed polarizer configuration (Figure 2).

2.2 Deformation of Liquid Crystals

If an electric field reorients the director, energy is being put into the system, disturbing it from its equilibrium state – the preferred state of lowest free energy. Since it has a semi-crystalline structure, the elastic forces of Hooke's Law apply to LCs.[6] From this assumption, the free elastic energy, ω_F, can be written using the Frank-Oseen model:

$$\omega_F = \frac{1}{2}K_1(\nabla \cdot \hat{n})^2 + \frac{1}{2}K_2(\hat{n} \cdot \nabla \times \hat{n})^2 + \frac{1}{2}K_3|\hat{n} \times \nabla \times \hat{n}|^2$$

$$+\frac{1}{2}(K_2 + K_4)\nabla \cdot [(\hat{n} \cdot \nabla)\hat{n} - (\hat{n} \cdot \nabla)\hat{n}]$$

where the variables $K_1,\ K_2,\ K_3,\ K_4$ are material properties known as the Frank constants[8] and have a magnitude on the order of 10^{-11} N/m.[6] The terms in this model correspond to the energy due to splay, twist, bend, and saddle-splay, respectively.[8]

The LC cell configuration that we consider here is the geometry known as a Fréedericksz cell. This cell consists of two parallel, electrically conductive glass microscope slides separated by a small gap (approximately 10 microns) that is filled with LC material. The device creates an electric field across the LC sample when a voltage is applied across the slides. Molecules lying close to the slides are strongly anchored by steric interactions with polymer coating on the slides. This polymer coating is applied to promote uniform LC order within the Fréedericksz cell for repeatable results.[9]

When an electric field is applied across a Fréedericksz cell, a LC can rotate from its preferred equilibrium state. To overcome the equilibrium state and set the LC into motion, the applied electric field, which imparts a torque to the LC molecules, must exceed a critical electric field, E_c, known as the Fréedericksz transition. Solving the Euler-Lagrange equation resulting from a variation of the free energy yields a solution[2] for this critical field in terms of the permittivity, ε_0, splay elastic constant and the thickness of the LC medium, d:

$$E_c = \frac{\pi}{d}\sqrt{\frac{K_1}{\varepsilon_0 \Delta\varepsilon}}$$

Since a Fréedericksz cell acts as a parallel plate capacitor, this critical field can be related to a critical voltage, V_c, through the equation:

$$V_c = E_C d$$

The Fréedericksz transition happens at approximately 1V for 5CB[10] and can optically be observed by observing the change in the refractive index of the material. For large fields, this change in refractive index approaches $\Delta n = n_e - n_o$, while for smaller changes it is approximately:

$$\Delta n = \frac{n_e({n_e}^2 - {n_o}^2)}{{n_o}^2}\frac{E - E_c}{E_c}$$

On a LC device this change in birefringence manifests as varying intensity of the transmitted light. Thus, the transmitted light will have different optical properties while under different strength fields.[2]

2.3 Liquid Crystal Dynamics

Since LCs exhibit both solid and fluid properties, both elastic and viscous forces are at play during perturbations. To create fast-switching LC devices the rotational viscosity should be minimized. This quantity can be written in terms of temperature and the order parameter, with

the activation energy, E', the Boltzmann constant, k_0, and a constant of proportionality, b, as constants.

$$\gamma_1 = bSe^{E'/k_0T}$$

From this equation it is clear that as temperature increases, the rotational viscosity decreases rapidly. This implies that keeping a stable temperature when measuring LC dynamics is important.[4] If the temperature increases beyond a certain point, the rotational viscosity becomes sufficiently small that thermal Brownian fluctuations dominate and destroy orientational ordering.[7]

As the LC switches, the transient phase change due to birefringence can be approximated as exponential decay function.

$$\delta(t) \cong \delta_0 e^{(-2t/\tau)}$$

Here, δ_0 is the initial phase of the light transmitted through the cell. The steepness of this transient response is due to the time constant, τ, which is different for forced switching due to an applied external field and for the relaxation of the LC to its preferred state from a perturbed one.[4] The values for these different time constants are given by the equations:[11]

$$\tau_{on} = \frac{\gamma_1 d^2}{\varepsilon_0 \Delta\varepsilon\left(V^2 - V_c^{\,2}\right)}$$

$$\tau_{off} = \frac{\gamma_1 d^2}{\pi^2 K}$$

From these equations we can determine that the time constant associated with the switch-on can be varied with the voltage of the applied field. For the switch-off, the material properties of the device, such as K, define the switching time constant.[11]

$$K = K_1 + \frac{K_3 - 2K_2}{4}$$

The observed intensity change during this transition as observed through cross polarizers can be approximately defined in terms of time.[4]

$$I(t) \cong sin^2\left(\frac{\delta(t)}{2}\right)$$

2.4 Carbon Nanotubes and Liquid Crystals

Colloidal suspensions of nanoparticles in a LC medium have been heavily investigated in recent years. Nematic LCs have been shown to transfer their long-range orientational order onto the nanoparticles.[12] It has been hypothesized that the addition of nanotubes could lead to a reduction in the Fréedericksz transition,[13] which could explain experimental results in which a CNT-doped cell requires less DC voltage to switch.[11,14] One analysis of the dynamics of this variation suggested that CNTs could also marginally improve LC time to reach peak transmittance in response to 1 kHz AC signals above 20 V.[15] Additional studies have probed the response to DC voltages and found similar results.[14] However, the promise for switching enhancement with LC doping remains largely unexplored.

3. Methodology

3.1. Polarized Light Microscopy

In order to study the switching dynamics of LCs, high-speed imaging and polarized light microscopy were employed. Polarized light microscopy involves the use of a light microscope, a polarizing filter, and an analyzer. As seen in Figure 2, light from a variable power LED source was used to illuminate the samples, whereby transmitted light was focused onto a high-speed camera via a Nikon S Plan Fluor ELWD 20× magnification objective lens with a working distance of 6.9 to 8.2 mm. Non-polarized light from the LED is polarized by a linear polarizer, before reaching the sample. After passing through the sample, it encounters a second linear

polarizer (analyzer), which is aligned perpendicularly to the polarizer. Thus, if the sample provides no retardation to the incident light, no light is transmitted to the camera. However, when a retarder is positioned between the cross polarizers, such as a LC device, the polarization state of the light is changed. Because of the birefringent properties of LCs, they act as variable retarders, and the orientation of the bulk LC phase can be probed by observing the change in light transmission to the camera. Incident light propagates at different speeds through the medium, relative to the anisotropic refractive indices of 5CB. The resultant intensity as it is seen by the camera is given by the equation:

$$I(\theta, d, \lambda, \Delta n) = I_0 sin^2 2\theta sin^2 \left(\frac{\pi d}{\lambda}\Delta n\right)$$

The observed intensity of a LC during a switch is primarily a function of the orientation of the director with respect to the polarizer, θ, with the constant variables of initial intensity, thickness, and birefringence of the sample (I_0, d, and Δn respectively) and the wavelength of light, λ, factoring into the observed intensity as well.[6] Application of an electrical field to these materials can cause the switching behavior of LCs to be induced and the resulting change in transmittance can be recorded by video using polarized microscopy.

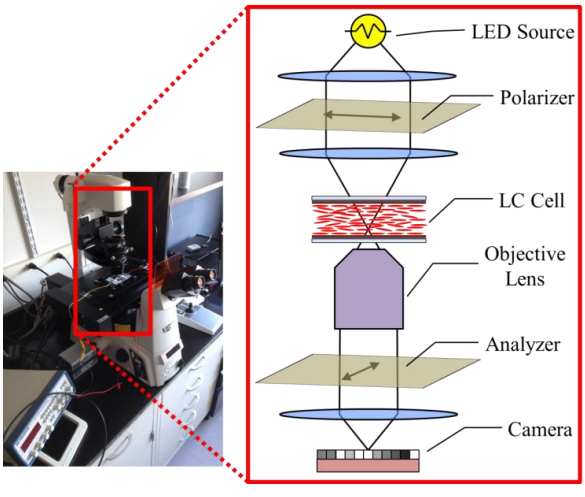

Figure 2 – Schematic of Polarized Light Microscope: Light from an LED source is polarized and then focused on the LC cell. The objective lens collects this light and it passes through a cross polarizer before reaching the camera.

Polarized light microscopy is a well-established diagnostic method for characterizing LC devices statically. The addition of a high-speed camera enables the imaging of LC dynamics by rapidly quantifying the state of the LC during the transition. This setup yields grayscale images that are proportional to the local transmitted light intensity through the sample. Unlike existing methods for studying LC dynamics, this method provides the access to both spatial and temporal changes in the LC medium.

Since the switching time of LCs is known to occur on the order of about 100 milliseconds, the apparatus requires a camera with sufficiently high frame rate to capture this process and avoid aliasing. An Andor Zyla sCMOS camera, able to achieve rates of up to 1000 frames per second, was used in conjunction with a Nikon Eclipse Ti microscope. For observation of LC devices in this study, a CoolLED pE-100 was used to illuminate the sample. For observation of LC devices in this study, an objective lens of 20X magnification was used to collect images of 128x128 pixels, corresponding to a viewing window of 41.6 x 41.6 μm^2. This small experimentation window was used to boost the frame rate and allow for faster imaging. A global shutter was employed with a 12-bit pixel field. The exposure of a single frame was 1.3 milliseconds. With this configuration, videos of LC switching were taken at approximately 715 frames per second meaning that each frame was separated by only about 1.4 milliseconds.

3.2. Control of Liquid Crystal Switching

Each Fréedericksz cell device was created by using capillary action to fill a prefabricated liquid crystal cell (PYSER-SGI 9136) with 5CB LC (TCI). These LC cells were manufactured to have a sample thickness of 10 microns. Briefly, the interior surfaces of the cell were coated with a thin layer of Indium Tin Oxide (ITO) to give them a conductive layer, as seen in Figure 3. The conductive ITO layers were spin coated with a layer of polyimide (PI). The PI layer of each

slide was directionally rubbed to create microscopic grooves in the PI layer, which promote LC director alignment along the rubbing direction. These rubbing directions of the top and bottom substrates were arranged in an antiparallel orientation.

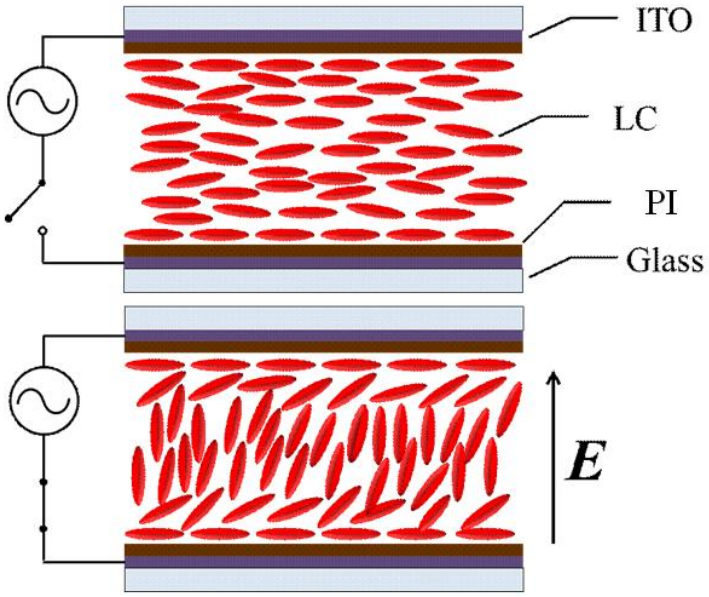

Figure 3 – Cross Sectional Schematic of a LC Cell: Top, the different layers of a LC cell (not to scale) are labeled. Electrodes are attached to the conductive ITO layer but the circuit is open so no electrical signal. The molecules are in a semi-ordered alignment and more light is transmitted in this arrangement. Bottom, the circuit is closed and an electric field is induced, forcing the molecules to align vertically. Less light is transmitted in this orientation.

The cells filled only with 5CB are generally referred to as "neat" due to the lack of any dopants. CNT doped cells were also prepared in a similar manner, except that prior to filling the device, multi-walled CNTs (MER Corporation) were added to 5CB at 0.01% by weight. These CNTs were produced by catalytic chemical vapor decomposition and measured approximately 7 microns long and 140 nm in diameter. This mixture was then sonicated for 30 minutes to disperse the CNTs before finally adding the LC/CNT suspension to the device. To avoid aggregation of the CNTs over time, the devices were tested immediately after loading. To test the uniformity of the thickness and LC alignment, the completed cells were held up to a light box with a polarizer. If the transmission was uniform in intensity across the center of the cell, it was

deemed acceptable and used in experiments. While this research studied 5CB, the experimental methodology could easily be extended to study the dynamics of other types of LCs or variable retarders.

To control the switching of the LCs a Rigol DG1032 30 MHz function generator was used to create a tailored waveform pattern. Two modes of operation were used to trigger switching in the Fréedericksz cells: an AC voltage and a DC voltage. Because the goal of this work was to examine the transient behavior as the LCs are forced to switch or relax, a signal with a square wave envelope was applied generating both the switch-on and switch-off processes over 10 cycles while a high-speed camera acquired image data.

For measurements using DC voltage the square wave simply switched between the voltage maximum (varied in a range between 2 and 8 V) and zero voltage. For AC forcing, a sine wave signal of chosen frequency (varied logarithmically between 0.1 and 100 kHz) was modulated by a square wave envelope to produce a modulated pulsing signal to control the electric field. In other words, one pulse from this machine consisted of a high frequency signal at a chosen peak-to-peak voltage ($V_{p\text{-}p}$) amplitude (varied in a range between 2 and 15 V) followed by a signal of zero volts, each applied for the same specified time interval (1 second). This signal was applied to the sample via flat-jawed alligator clips to increase the contact area between the conductive ITO layer and the leads to the function generator. The integrity of the signal was verified using a Rigol DS1104 oscilloscope.

This process resulted in the LC being forced into the aligned and relaxed states respectively. Since 5CB has consistent nematic behavior up to 35°C [7], and because trials took no more than half a minute with a 50% duty cycle, the thermal effects on the LC by this electrical pulsing are negligible.

3.3. Data Analysis Techniques

After obtaining the raw video files, image processing was performed to extract quantitative information about the dynamics of the LC switching process. Using custom image analysis software written in Matlab, each individual frame of a video was opened and the mean and standard deviation of the pixel intensity across the image was computed and stored. As we expect a uniform response of the LC director in the Fréedericksz cell geometry, it was not necessary to analyze spatial variations in the image data. By monitoring these values over the length of the video, which typically included approximately 10 switching cycles, information about the orientation and uniformity of the bulk LC orientation during the switching process was extracted.

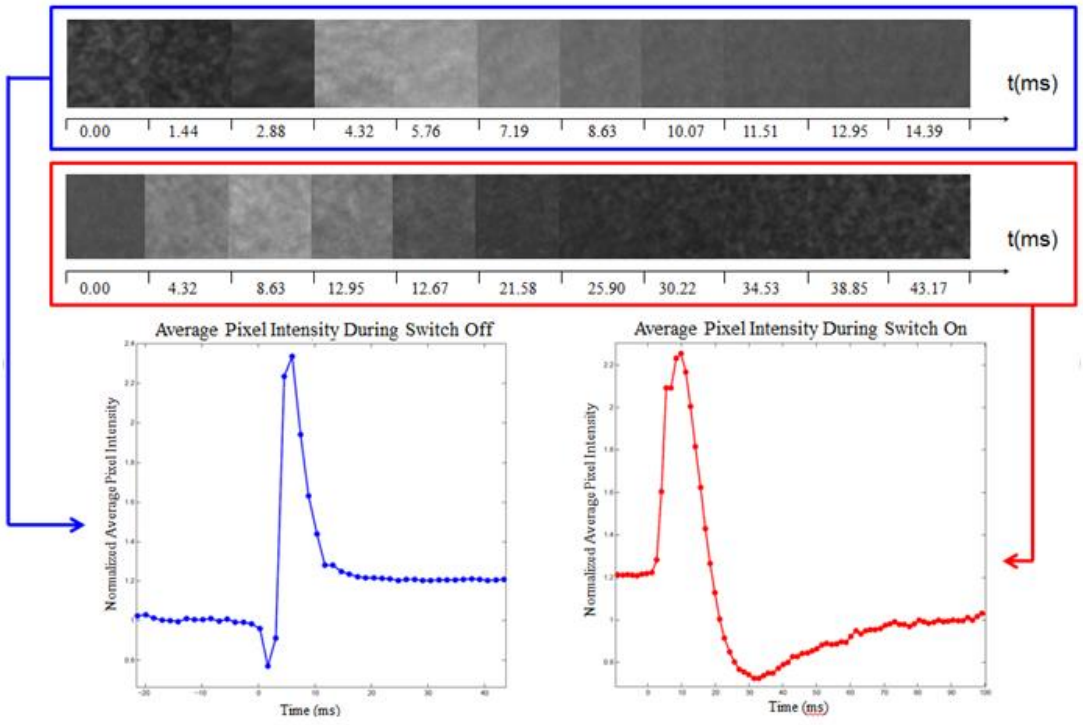

Figure 4 – Sample Video Showing Switching Process and Intensity Mapping: The frames at the top of this figure are displayed across a time axis to give the sense of how a video looks over time. This raw data is processed and the average image intensity is examined over time resulting in the plots shown at bottom.

After data acquisition, further analysis was conducted to determine the amount of time needed for the LC to switch and subsequently to relax (Figure 4). This was accomplished by creating a time series of the transmitted light intensity and measuring the deviation of the instantaneous intensity from the steady-states on and off values. The switches were defined by the times when the intensity, $I(t)$, was between 95% and 5% of the steady state off, I_{off}, and on, $I_{on,}$ intensity range. These values correspond to $I(t)/(I_{off}\text{-}I_{on}) = 0.95$ and $I(t)/(I_{off}\text{-}I_{on}) = 0.05$, respectively. The algorithm that was used to uncover this information is outlined in more detail below. To promote modularity in functionality, a number of constants "k" were selected for algorithm performance and statistical measurement. The values for these constants can be referenced in Table 1.

1. Since each video had more than ten switching cycles in it, it was first segmented into ten sections, each highlighting one pulse from the electrical signal. In each section, both switches could be seen in their entirety so the characteristics of each switch could be quantified separately. Thus, the data reported for each video was comprised of aggregated data from each of these pulses. The pulses were parsed in a semi-automated manner, by manually selecting a starting point for the first pulse. This starting point was chosen as a point when the LC was in the off steady-state prior to switching. From this point the pulses were cropped from the full signal with duration of the number of seconds in the period of the pulsing. Time was determined for each frame *i* using the video frame rate *fps* in the following equation:

$$t_i = i * fps$$

2. Due to the inherent noisiness in the data caused by Brownian fluctuations of the LC director field and oscillations from the AC driving voltage, a smoothing algorithm was

employed on each pulse to regularize the data. This was done using a central moving average with a smoothing window of k_0 frames.

3. The difference between steady-state intensities was crudely calculated by quantizing the data into k_1 discrete bands. This very rough smoothing algorithm ensured that the approximate values of the two steady-state intensities could be determined by finding the two most frequent values of this discretized data. The "steady-state tolerance," used later in the algorithm was defined as $1/k_2$ times the difference between these intensities. For experiments where this step resulted in the same number for the steady-state of both orientations, this step was skipped and a 'steady-state tolerance' of k_3 was used globally.
4. Steady-state intensity thresholds for both the "on" and "off" orientations were then determined. Since each segmented pulse began in the off position, transitioned to the on position and then back off, the first few hundred frames of each segment represented the steady-state intensity of the LC in the off orientation. The average intensity was iteratively calculated using a cumulative moving average starting with the first k_4 frames of the pulse and incrementing the range of frames used in calculating this number. The steady-state off state was defined by this average after the final point in the set exceeded the steady-state tolerance. The same iterative process was used to highlight the steady-state on state intensity, where the starting point for the average being midway through the pulse instead of being at the beginning.
5. Because the intensity of the LC devices with no voltage signal was the same across all trials, the intensity data for each frame was normalized by dividing through by the steady-state off intensity.

6. To highlight the switching process, each frame of the video was examined. The first frame to exceed k_5 of the distribution for the steady-state set was defined as the starting point for the switch. The end point was set where the step response had settled to within k_6 of the opposite steady-state intensity. The set of data points comprising the switch consisted of all the data between these points. The duration of the switching process was determined by multiplying the frame rate by the number of frames in the switch.

Variable	Constant Selected
k_0	15
k_1	100
k_2	10
k_3	0.5%
k_4	10
k_5	2σ
k_6	5%

Table 1 – Table of Constants: While analyzing data during this research, the variables above were used to promote easy alterations to the algorithm. The constants above were assigned to these variables as they worked well with the generated data, but other constant combinations may be more effective for different applications. σ represents one standard deviation of a normal distribution.

3.4. Design of a Rotation Stage

Because the LC Fréedericksz cell acts as a retarder, its angle relative to the polarizer affects the amount of light transmitted through the analyzer and thus to the camera. In order to adjust this angle, a custom rotation stage was designed and fabricated. Since the microscope's focal plane was precisely positioned within the 10 micron thick LC sample, the stage insert needed to have a tight flatness tolerance of ±0.02" to accurately image a cross section of the device. Furthermore the device had to be sufficiently thin so that the sample did not sit above

the focal plane of any of the available objective lenses. Secondly, the fixture needed to be positioned at different angles to the polarizer. The rotation stage was also required to accommodate microscope slides of different sizes and to allow electrical leads to be connected to the sample without short-circuiting. Finally, the rotation stage insert was required to apply a small clamping force to the LC device so that it would remain parallel to the focal plane.

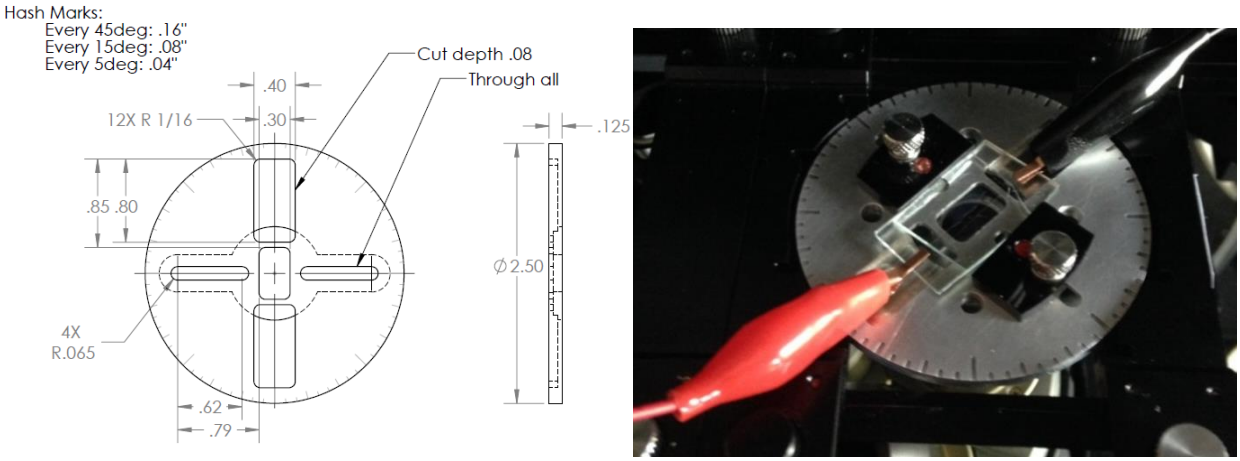

Figure 5 – Rotation Stage Design and Fabrication: Left, engineering drawings dimensioning and tolerancing a rotation stage insert to meet the required specifications. Right, the final part was CNC machined from aluminum and is shown sitting in the microscope stage with a sample connected to electrical leads

The part was designed and fabricated (Figure 5) from a 1/8" sheet of precision ground aluminum due to its ease in machining and flatness. The insert was circular in order to fit inside an existing microscope stage and allow for easy rotation. Hash marks were machined on the edge of the insert in five degree increments to provide a reference angle. Slots were cut out so that sliding beveled clamps could clamp the LC device securely in place by providing a slight downward force, while maintaining parallelism to the stage. Relief cuts were made perpendicular to these slots to allow for insulated electrical leads to attach onto the conductive glass without touching the stage and causing a short circuit. The insert was thin enough to be viewed on objective lenses up to 40X with a working distance of 2.8 – 3.6 mm.

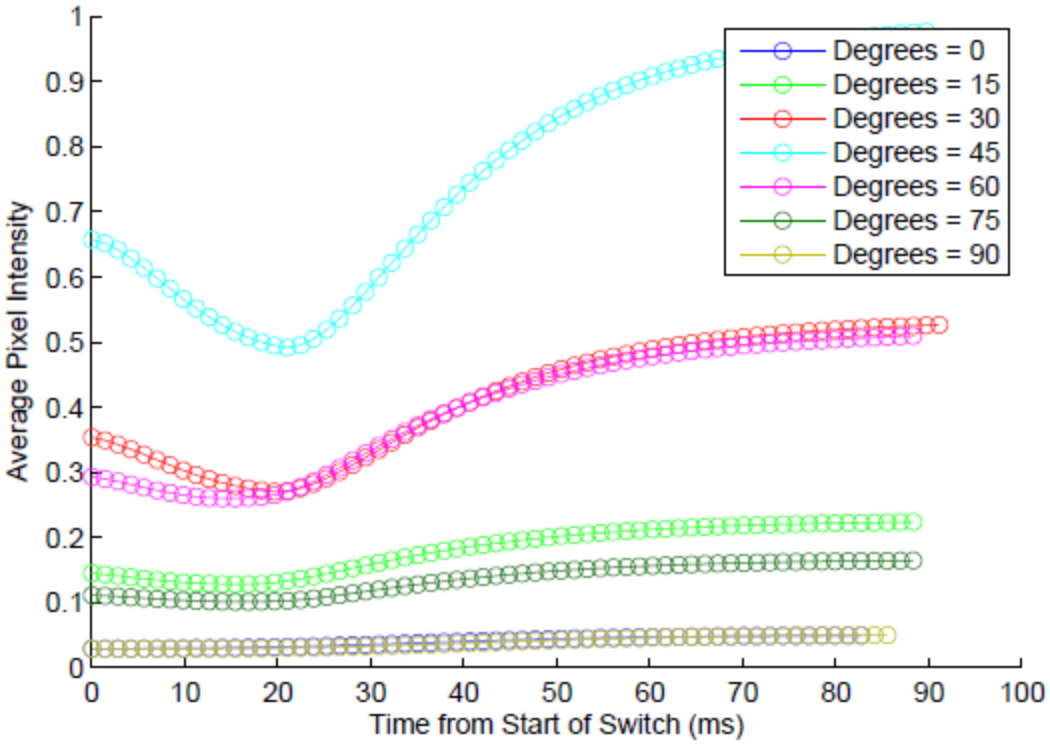

Figure 6 – Transmission Intensity for LC Cell at Different Angles: To determine the maximum transmission position of LC cell, an experiment was conducted varying the angle of the LC to the polarizer. From the plot, it is clear that an angle of 45° is optimal. This finding is corroborated by existing LC theory.

An experiment was conducted to determine the angle for maximum light transmission in order to take videos with the highest contrasts. By varying the rotation stage angle and processing the intensity seen during each switch, the angle of 45° was shown to be the best position for experimentation (Figure 6). As a result, the orientation of the cell was adjusted for maximum transmission in the off state before each experiment, which corresponded to approximately 45° relative to the polarizer.

4. Results and Discussion

4.1 Validation of High-Speed Polarization Microscopy

To validate the efficacy of high-speed polarized light microcopy as a viable method to study LC switching, a series of tests were conducted on a well characterized LC material and

device. 5CB LC was switched in a Fréedericksz cell, in which the voltage of a 100 kHz AC signal was varied. Trials were conducted using a base signal with a square wave envelope with a period of 2 seconds, a frequency of 100 kHz for the underlying sine wave, and a variable $V_{p\text{-}p}$ of 2, 2.5, 3, 5, 10, and 15V. Aggregating data across ten pulses, the average pulse was determined and the intensity profile during the switching process was plotted (Figure 7) for each condition and for both the switch-on and switch–off transitions.

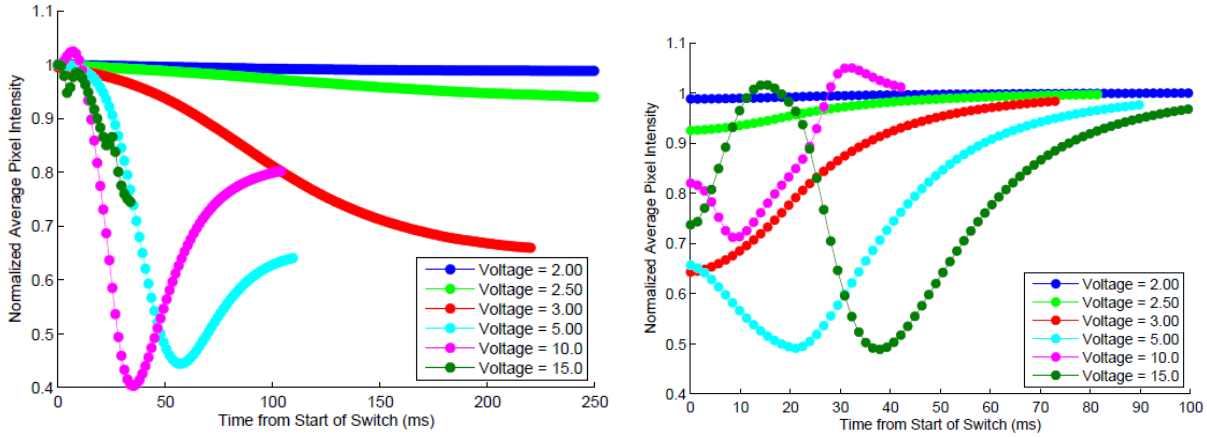

Figure 7 – LC Switching Dynamics as Voltage is Varied: Left, when the circuit is completed, The LC device switches from the relaxed off state to alignment in the on state; right, the LC switch from the aligned state into the relaxed off state as the circuit is changed from closed to open.

From these plots, several trends are clearly observable. First, the steady-state intensities with the voltage on and off differ from one another, an effect which can be seen in Figure 8. The plots above are normalized to the steady-state off intensity. Second, the steady-state intensity when the voltage is on varies with the voltage input, implying that the steady-state director orientation of the LCs is dependent upon applied voltage. This corresponds well with LC theory, which also predicts that the birefringence and hence retardation of a sample changes with the strength of the applied external field.

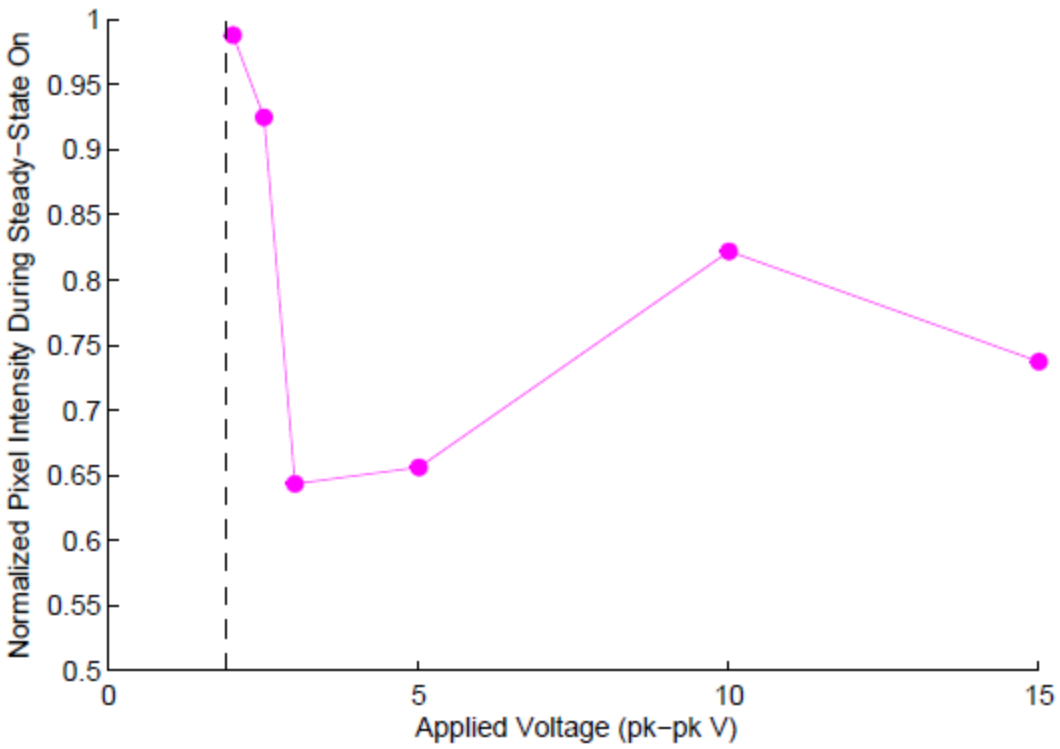

Figure 8 - Effect of Voltage on Steady-State Transmission Intensity: The steady-state intensity while the electric field was active was variable along with voltage. The most light was transmitted closest to the Fréedericksz transition as there was the least impetus for change in orientation from the highly transmissive off state. Error bars for each data point are shown.

Furthermore, the time scales for the switch-on and switch-off transitions are not equal. This difference stems from the different forces that are at play, driving each process. In the switch-off event where the circuit goes from being closed to open, the driving force for the transition is the entropic LC rearrangement to minimize its configurational energy. For the switch-on however, electrical energy is being poured into the LC sample, forcing it into alignment with the field. When analyzing LC switching dynamics, it is important to consider each switch as a separate process because of these different forces.

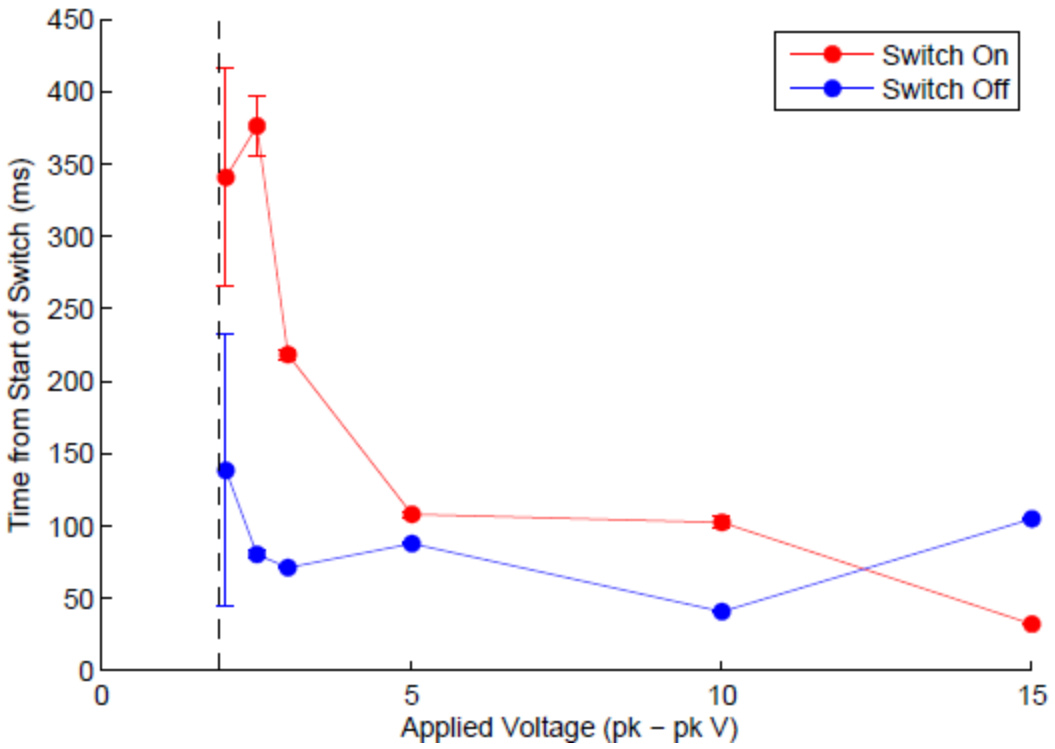

Figure 9 – Switching Time as a Function of AC Voltage: Switching times for both switches decay from a vertical asymptote at the Fréedericksz transition as the voltage increases. Error bars are shown. The dashed line represents the Fréedericksz transition for 5CB.

For the trials in which the input AC signal voltage was varied, the switching time decreased with an increase in voltage for a fixed frequency (100 kHz). At low voltages near to the Fréedericksz transition the bulk LC experiences little force from the electric field and as a result is not displaced far from its preferred relaxed state orientation. For the switch-on, this weak force requires a longer time to force the LC to its final state, as compared to the switch-off. At higher voltages a greater torque on the LC molecules results in faster switching time. As the voltage is increased above the Fréedericksz transition the switch-on time generally exhibits exponential decay. According to LC theory, the time constant of the switch-on has an inverse square relationship to the applied voltage above the critical value, and this relationship is visualized in Figure 9.[11]

$$\tau_{on} = \frac{\gamma_1 d^2}{\varepsilon_0 \Delta\varepsilon \left(V^2 - {V_c}^2\right)}.$$

For the switch-off, the time required to switch is roughly constant across all voltages. Since the time constant for this process depends on material properties that do not change dramatically with the switching constant, the rate of switching for the switch-off is largely constant across different voltages as implied by the equation:[11]

$$\tau_{off} = \frac{\gamma_1 d^2}{\pi^2 K}$$

That these low resolution results for a standard 5CB Fréedericksz cell correspond with well-established LC experiments, simulation and theory shows that the method of polarized light microscopy is probing the orientation of these devices and providing accurate measurements. Using this methodology is an effective way to compare performance characteristics of different cells under forcing conditions.

4.2 Liquid Crystal Response to AC Forcing

To determine the effects of CNTs on LC switching dynamics, a series of measurements were performed on neat 5CB LC devices and compared directly to 0.01% CNT doped 5CB devices. The switching dynamics of these two cell types were tested at various AC voltages and frequencies. The voltage of the input signal was varied from 3 to 9 V, by 2V increments. The frequency parameter varied by starting at 0.1 kHz and logarithmically increasing the frequency by a factor of 10 until 100 kHz.

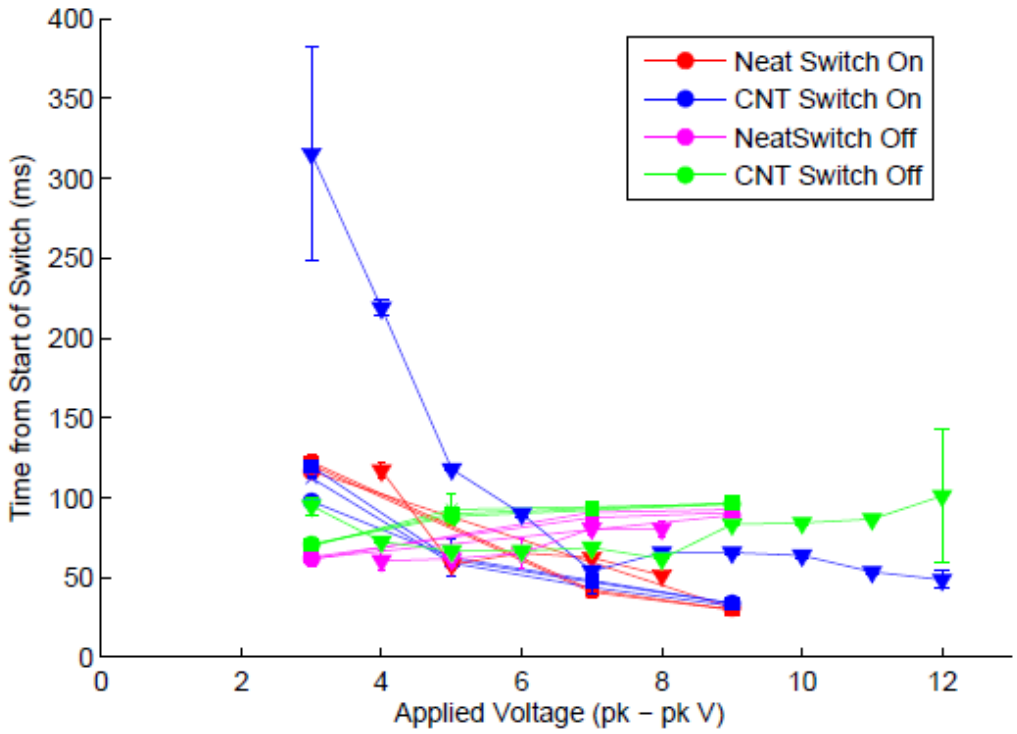

Figure 10 – Switching Times of Neat and CNT Cells at Low Frequencies: Both cells were tested at 0.1, 1, 10, and 100 kHz. The markers corresponding to each of these symbols are ●, **x**, ■, and ▼ respectively. As seen in this chart, varying the frequency in this range produces little change. Trials that could not be analyzed by the algorithm outlined in section 3.2 were omitted from this plot. Error bars are shown.

From Figure 10 it is apparent that the data can be divided into two regimes, the low frequency (0.1 – 10 kHz) and high frequency (100 kHz) regimes, shown separately in Figure 11. Varying the frequency in the low range produced almost no change in LC behavior. From this data, it is clearly apparent that the addition of CNT particles did not enhance the LC device's switching speed. The frequency of 100 kHz dramatically changed the LC-CNT suspension behavior, where the switching time grew dramatically as the voltage decreased. LC devices are most commonly switched using very high frequency signals, so this trial was of particular interest. The voltages tested were in the range 2 to 12 $V_{p\text{-}p}$, testing signals at 1 V intervals. In the high frequency regime, the use of CNTs as a dopant only slowed the switching process for all tested voltages.

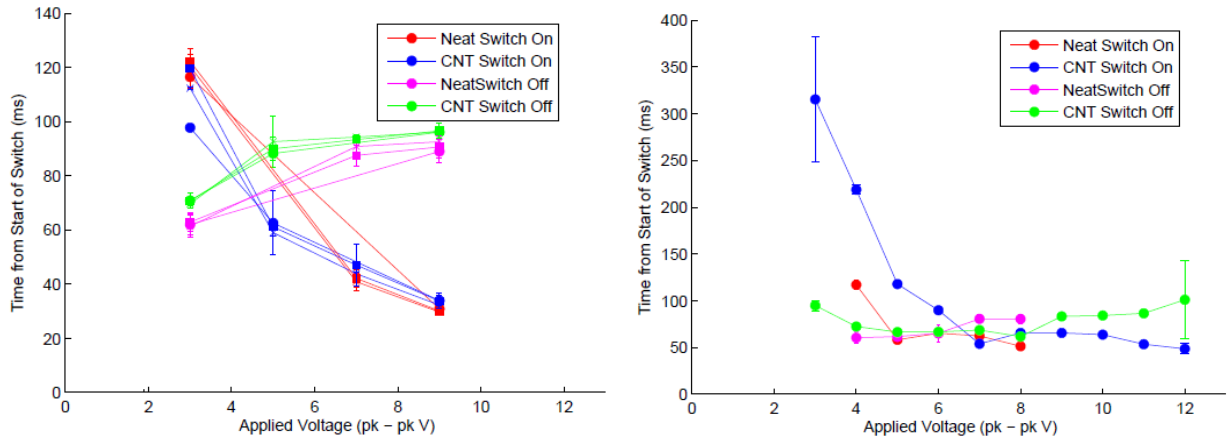

Figure 11 – Switching Times of Neat and CNT Cells at 100 kHz: Left, in the low frequency regime variation in frequency does not change the liquid crystal switching dynamics. The markers corresponding to the frequencies of 0.1, 1, and 10 kHz are ●, **x**, and ■ respectively. The addition of CNTs has no effect on the switching time. Right, in the high frequency regime AC voltage is increased, and the switching time of the LC cells decreases. CNTs impede switching at low voltages, but show slight improvement at higher voltages. Error bars are included in both plots.

The results from this series of tests are similar to those conducted in the preliminary testing of LC devices in section 4.1. At voltage levels close to the Fréedericksz transition, the switching time increases significantly. As the voltage is increased, the switching stimulus becomes greater and the switching time dramatically decreases. The addition of CNTs has a limiting effect for the lower voltages, while it has almost no effect at higher voltages. In this scenario, the CNT acts as a large metallic rod compared to the smaller LC molecules. Without a sufficiently high voltage, the CNTs impede the switching of the LC.

4.3 Liquid Crystal Response to DC Forcing

Neat and CNT cells were driven using DC voltage, and the results changed significantly compared to the AC case. In this series of experiments, the voltage was varied from 1 to 8 V with 0.5 V increments. Switching using DC voltage tended to take longer than with AC voltage, so a 4 second period was used with a 50% duty cycle, leaving the voltage to alternate between high and low for 2 seconds at a time. To avoid ion flux effects from running DC voltage unilaterally through the cell, trials were alternated between a positive and negative voltage

signal. Running a LC device with DC voltage is not a common practice because such a stimulus could cause unfavorable ion transport and trapping across the device.

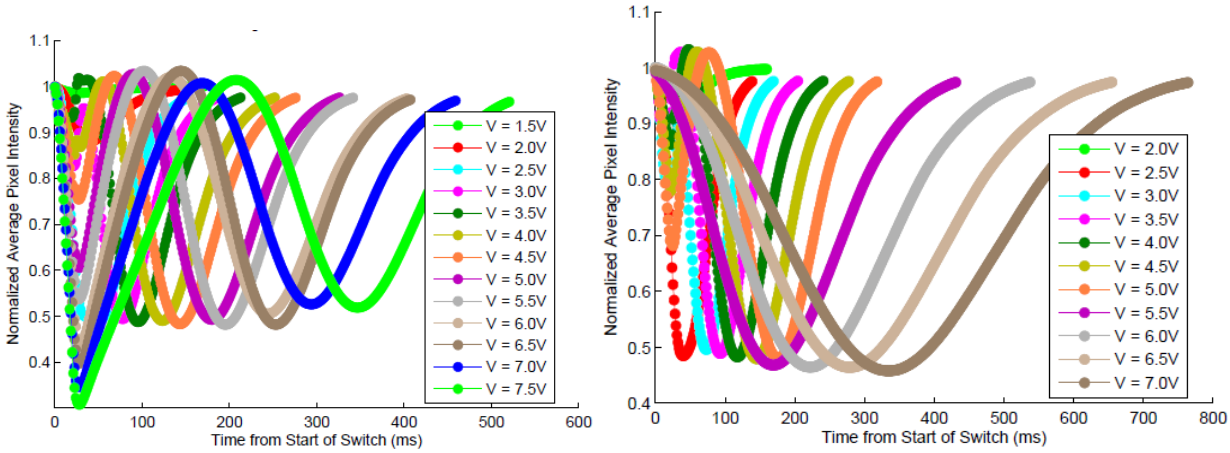

Figure 12 – Switching Induced by DC Signal: From left to right: the switch-off from the CNT cell; the switch-off from the neat cell. It is clear in both plots that there is not a transmittance change between the on and off steady-states of the cell.

An interesting phenomenon found when testing DC voltage was that for both neat and CNT cells the steady-state on and off intensities did not differ from one another, an effect which is illustrated in Figure 12. This phenomenon has been observed for LC cells when they are tested with sufficiently low frequency or DC signals.[16]

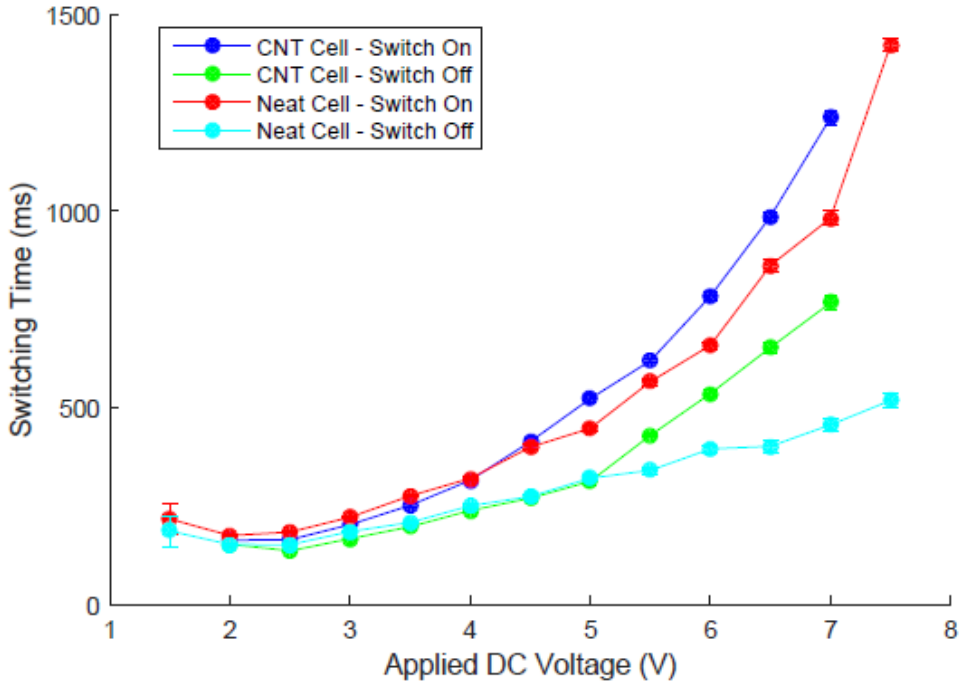

Figure 13 – Switching Times of Neat and CNT Cells from DC Signals: As voltage is ramped up, the switching time generally increases for all voltages, with a minimum around 2.5V. The addition of CNT particles slows switching down at higher voltages. Trials which switching could not be accurately highlighted were omitted from this plot. Error bars are plotted.

Figure 13 demonstrates that CNTs hinder the switching dynamics of LCs at higher voltages for both the switch-on and switch-off processes. For both neat and CNT cells, as the voltage is increased, the switching time rapidly increases. Between the Fréedericksz transition and approximately 4 V, the addition of CNTs to the LC cell decreased the switch-on time by 10%. The switch-off saw similar trends in performance up to 5 V. This effect could potentially be amplified if investigated further by varying the concentration of CNT particles in 5CB to find a local maximum.

Above the critical voltage, in the high voltage regime for each switching process, the CNTs slowed down the switching time considerably as shown in Figure 14. As the voltage is increased, the percent difference in switching time between neat and CNT-doped LC devices becomes increasingly negative. Carbon nanotubes are on the order of 1000 times larger than LC

molecules and have considerably more inertia than the smaller molecules around them. In contrast to the LCs, the CNTs behave as metallic particles, and they are unaffected by the applied external field. Thus, the CNTs must be rotated i by the torque supplied by the surrounding LC molecules, which are likely slowed due to the hydrodynamic resistance of the CNT. By varying concentration and voltage, one could potentially maximize the performance gain seen by switching the cells at low voltages.

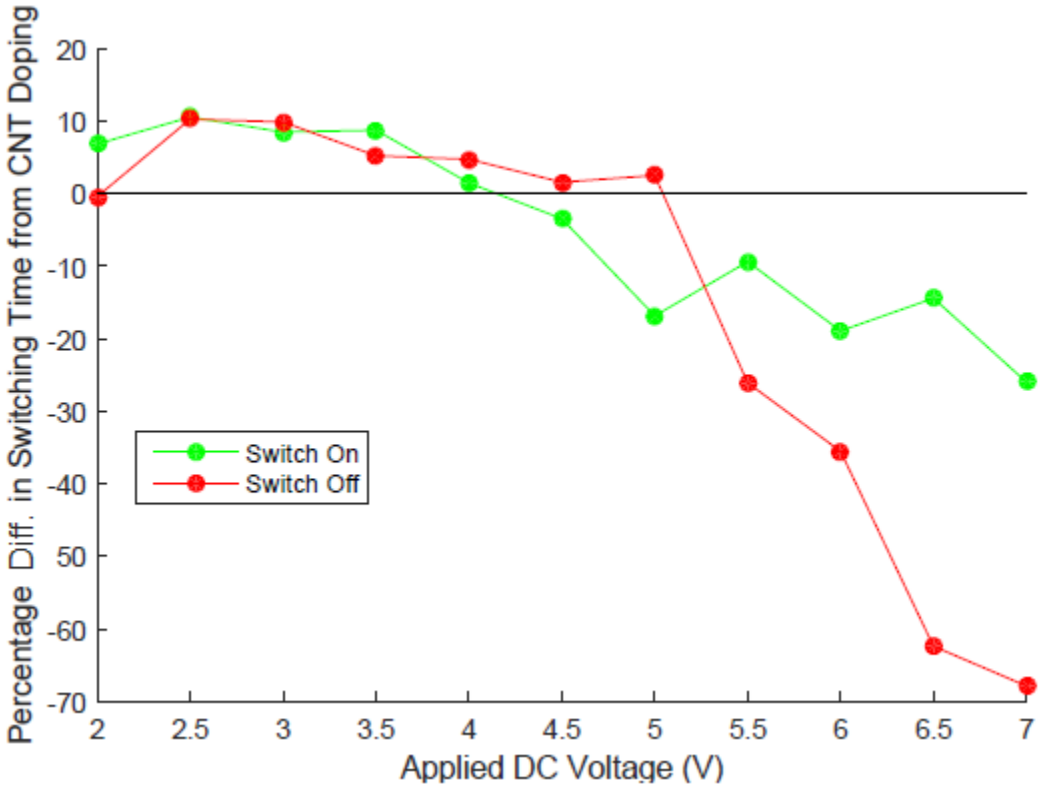

Figure 14 – Switching Speed Percent Difference due to CNT Doping: A positive percentage difference corresponds to the CNT dopants decreasing response time and improving performance. While the DC voltage was low, the addition of CNT dopants improved performance of the 5CB LC cell up to 10%. Under higher voltage signals though, the addition of CNTs had the opposite effect, slowing the device considerably.

5. Conclusion

High-speed polarized light microscopy has been shown to be a simple and robust method for analyzing LC switching dynamics. This method is capable of providing temporal maps of transmission intensities, with the potential for spatial resolution as well. The experimental data

gathered on 5CB performance over a series of driving voltages in a Fréedericksz cell geometry demonstrates the consistency of our measurements with existing research.

The high-speed imaging method was then used to measure the effects of CNT dopants on LC switching dynamics. CNT-doped cells were found to improve device switching times by about 10% at 2.5 – 3.5 V. At high voltages (V > 5V), CNTs inhibited LC switching time and impeded the process of switching without bound as the voltage was increased. More study is warranted to determine if CNTs can be exploited produce faster switching LC devices.

The experimental variable of CNT dopants is representative of many of the possible factors that could be altered to improve performance. The novel method of polarized light microscopy to study this effect can be extended to study the effects of other variables when diagnosing LC switching. Future work should use this method to test these parameters to rapidly explore other configurations that could lead to enhanced device performance. Furthermore this data can be analyzed through spatial image processing to resolve the LC switching process in both the spatial and time domains.

6. Acknowledgements

I would like to personally thank everyone who supported and contributed to my research at Tufts University. In particular, I would like to thank my advisor Prof. Jeffrey Guasto for his mentorship and guidance in this research and without whom this project could not have been possible. Prof. Timothy Atherton was instrumental suggesting this project guiding the research, and I thank him for sharing his extensive knowledge of liquid crystals. I would also like to thank Prof. Peggy Cebe and Matt Eakle, for sharing their resources and for assistance in fabrication of the LC cells. I appreciate the guidance provided by Jim Hoffman in designing and fabricating the rotation stage for the polarization microscope. Finally, I express gratitude to Yang Jin and

everyone else in the Liquid Crystal group at Tufts University for help and feedback on this project. Funding for this research was provided by the Summer Scholars program at Tufts University.

7. References

1. *LCD Industry Poised for Recovery as Forecast Tops $ 85 Billion Mobile PC / Tablet Shipments Remain Strong 2012 LCD TV Panel Shipment Growth Minimal*. (2012).

2. Andrienko, D. *Introduction to Liquid Crystals*. (International Max Planck Research School, 2006).

3. Selinger, R. L. B., Mbanga, B. L. & Selinger, J. V. Modeling Liquid Crystal Elastomers: Actuators, Pumps, and Robots. **6911,** 69110A–69110A–5 (2008).

4. Wang, H. *Studies of Liquid Crystal Response Time*. (2005).

5. Rahman, M. & Lee, W. Scientific Duo of Carbon Nanotubes and Nematic Liquid Crystals. *J. Phys. D. Appl. Phys.* **42,** 063001 (2009).

6. Hirst, L. S. *Fundamentals of Soft Matter Science*. (CRC Press, Taylor & Francis Group, 2013).

7. Belyaev, B. A., Drokin, N. A., Shabanov, V. F. & Shepov, V. N. Dielectric Anisotropy of 5CB Liquid Crystal in a Decimeter Wavelength Range. *Phys. Solid State* **42,** 564–566 (2000).

8. Adler, J. H., Atherton, T. J., Emerson, D. B. & Maclachlan, S. P. An Energy-Minimization Finite-Element Approach for the Frank-Oseen Model of Nematic Liquid Crystals: Continuum and Discrete Analysis. 1–31

9. Chen, R. H. *Liquid Crystal Displays*. (Wiley, 2011).

10. Hanmer, J. M. W. & Coles, H. J. Study of the Freedericksz Transition in 5CB Using Time-Resolved Raman Microscopy. *Mol. Cryst. Liq. Cryst. Sci. Technol. Sect. A. Mol. Cryst. Liq. Cryst.* **262,** 235–248 (1995).

11. Lee, K.-J. *et al.* Enhanced Electro-Optical Behaviour of a Liquid Crystal System via Multi-Walled Carbon Nanotube Doping. *Liq. Cryst.* **41,** 25–29 (2013).

12. Dierking, I., Scalia, G. & Morales, P. Liquid crystal-carbon nanotube dispersions. *J. Appl. Phys.* **97,** (2005).

13. Atherton, T. J. Influence of Carbon Nanotubes on the Freedericksz transition.

14. Lee, W., Wang, C. Y. & Shih, Y. C. Effects of Carbon Nanosolids on the Electro-Optical Properties of a Twisted Nematic Liquid-Crystal Host. *Appl. Phys. Lett.* **85,** 513–515 (2004).

15. Basu, R. Effect of Carbon Nanotubes on the Field-Induced Nematic Switching. *Appl. Phys. Lett.* **103,** 23–27 (2013).

16. Gathania, A. K., Singh, B. & Raina, K. K. Switching dynamics in ferroelectric liquid crystal mixture. *Jpn. J. Appl. Phys.* **43,** 8168–8172 (2004).